Letter

Stretched-exponential relaxation in weakly confined Brownian systems through large deviation theory

Lucianno Defaveri,[1] Eli Barkai,[2] and David A. Kessler[1]
[1]Department of Physics, Bar-Ilan University, Ramat-Gan 52900, Israel
[2]Department of Physics, Institute of Nanotechnology and Advanced Materials, Bar-Ilan University, Ramat-Gan 52900, Israel

(Received 22 September 2023; accepted 15 December 2023; published 6 February 2024)

Stretched-exponential relaxation is a widely observed phenomenon found in ordered ferromagnets as well as glassy systems. One modeling approach connects this behavior to a droplet dynamics described by an effective Langevin equation for the droplet radius with an $r^{2/3}$ potential. Here, we study a Brownian particle under the influence of a general confining, albeit weak, potential field that grows with distance as a sublinear power law. We find that for this memoryless model, observables display stretched-exponential relaxation. The probability density function of the system is studied using a rate-function ansatz. We obtain analytically the stretched-exponential exponent along with an anomalous power-law scaling of length with time. The rate function exhibits a point of nonanalyticity, indicating a dynamical phase transition. In particular, the rate function is double valued both to the left and right of this point, leading to four different rate functions, depending on the choice of initial conditions and symmetry.

DOI: 10.1103/PhysRevE.109.L022102

Introduction. Anomalous relaxation, characterized by nonexponential decay, is observed in a wide range of physical systems [1]. One class of such behavior is stretched-exponential relaxation [2–6]. This has been seen, for example, in disordered or heterogeneous systems, where the complex interplay of interactions leads to a broad distribution of relaxation times [7]. Moreover, the stretched-exponential behavior is observed in the particle movement in disordered dielectrics [8–10] and in the relaxation of glassy dynamics [11,12].

Some studies of the relaxation of ordered Ising ferromagnets have sought, building on the work of Huse and Fisher [13,14], to connect the observed stretched-exponential relaxation to an effective droplet dynamics, which was mapped to a Langevin equation with an $x^{2/3}$ potential [15]. It was shown that this model does indeed exhibit stretched-exponential relaxation. In this Letter, we present a solution to the Fokker-Planck equation with a general external potential that grows with distance as a sublinear power law. We show that for this class of models the relaxation of the various moments of the position to their equilibrium values follows an anomalous stretched exponential. Formally, the Fokker-Planck equation [see Eq. (2)] for $P(x,t)$, the probability density function (PDF), can be solved via an eigenfunction expansion, and yields stretched-exponential relaxation. However, it turns out that there is a simpler, more direct, approach, which also yields additional physical insight. We find that in the long-time limit, $P(x,t)$ takes the form of the exponential of a rate function which possesses a scaling form, as usually results from a large deviation formalism [16], which looks at the far tails of the distribution of an observable. Large deviation theory is a subject of much active interest in statistical physics [17–26], in particular, due to the recent discovery of dynamical phase transitions in the large deviation behavior of some model systems [27–34]. These are nonanalytic points of the rate function, and are so called due to the analogy of the rate function to an equilibrium free energy [20,22,29]. We show the relationship between the stretched-exponential relaxation and the presence of a dynamical phase transition.

The rate function is defined as the logarithm of the PDF $P(x,t)$, divided by a power of the time [20,21,29]

$$\mathcal{I}(z) \equiv \lim_{\substack{t,x\to\infty \\ z=x/t^{\gamma}\ \text{fixed}}} \frac{-\ln P(x,t)}{t^{\nu}}, \tag{1}$$

with the anomalous time exponent $\nu \neq 1$ and where $\mathcal{I}$ is a function of the scaling variable $z \equiv x/t^{\gamma}$. The stretched-exponential relaxation of observables will be governed by the same anomalous exponent ν. It should be noted that in the previously identified cases with anomalous temporal scaling, the observable in question was nonlocal in time, whereas here it is the PDF of x itself that exhibits the anomalous scaling. The appearance of a rate function in our problem implies the surprising result that the anomalous stretched-exponential relaxation we observe is a result of large deviations, i.e., the dynamics at large x.

We find that the rate function is multivalued, and possesses a critical point z_c. The rate function has two possible branches for $z < z_c$ and two for $z > z_c$, all meeting at z_c. All four possible combinations of branches below and above z_c have different interpretations, corresponding to different classes of initial conditions and parity. Two of the combinations have a jump discontinuity in $\mathcal{I}''(z)$, indicating the presence of a dynamical phase transition (see Refs. [22,29] for more details). Such a multivalued rate function appears not to have been encountered previously. Using the appropriate branches of the rate function, we obtain the timescales of the stretched-exponential relaxation of the even and odd moments of x.

Model. We study noninteracting Brownian particles, in contact with a heat bath at temperature T, that are also subject to a binding potential field $V(x)$. The spatial spreading of the cloud of particles can be described via the PDF $P(x,t)$, obtained from the Fokker-Planck equation (FPE)

$$\frac{\partial}{\partial t}P(x,t) = D\left[\frac{\partial^2}{\partial x^2} + \frac{\partial}{\partial x}\left(\frac{V'(x)}{k_B T}\right)\right]P(x,t), \tag{2}$$

where D is the diffusion coefficient. We consider herein even potentials, satisfying $V(x) = V(-x)$, which for large x grow as a sublinear power law, $V(x) \propto x^{\alpha}$, where $0 < \alpha < 1$. This means that the force, $F(x) = -V'(x)$, will be negligible for large x, as $F(x) \propto x^{\alpha-1}$. At long times, the particles will reach the stationary equilibrium Boltzmann-Gibbs state $P_{\mathrm{BG}}(x) = \exp[-V(x)/k_B T]/Z$, with Z being the normalizing partition function. For the more commonly considered superlinear growth of the potential, $\alpha > 1$, $F(x)$ grows with distance and everything is standard. The system exponentially relaxes to the Boltzmann-Gibbs state, at a rate given by the first nonzero eigenvalue of the Fokker-Planck operator, which has a discrete spectrum starting at 0. This discreteness follows from the fact that under a similarity transformation, the FPE becomes a Schrödinger equation [35] with an effective potential $V_S(x) = F(x)^2/4k_B T + F'(x)/2k_B T$, which grows without bound as $x \to \infty$. However, for $\alpha < 1$, $V_S(x)$ decays at large x as $x^{-2(1-\alpha)}$ and so the spectrum goes continuously down to 0. Potentials of this form have already been studied in the context of resetting processes [36] and active processes [37], in particular, the $\alpha = 1$ limiting case [38–40]. As noted above, in Ising ferromagnets below the critical temperature, the dynamics of spherical droplets have been modeled using an effective potential which, for $d = 3$ dimensions, is equivalent to $\alpha = 1$ and, for $d = 2$ dimensions, is equivalent to $\alpha = 2/3$ [13–15]. For $\alpha \to 0$ [and assuming $V(x) \sim x^{\alpha}/\alpha$], we have that for large x, $V(x) \sim \ln x$. In that limit, the relaxation has been shown to be governed by a power law [41–44]. The question is then what happens for $0 < \alpha < 1$?

For our numerical examples, we use the family of potentials

$$V(x) = V_0\left(1 + \frac{x^2}{\ell^2}\right)^{\alpha/2}. \tag{3}$$

For $x \gg \ell$, with ℓ being the length scale of the center region, the potential exhibits the desired power-law growth. Throughout this Letter, we shall scale the position variable by ℓ and correspondingly the time by ℓ^2/D.

As mentioned above, the $P(x,t)$ can be decomposed in a sum of eigenfunctions, each decaying as $e^{-\lambda t}$ with a continuous eigenvalue spectrum λ starting at 0^+, together with the Boltzmann-Gibbs bound state at $\lambda = 0$. It turns out that the dominant continuum contribution to $P(x,t)$ for large times comes from the vicinity of a particular finite eigenvalue λ_*. This dominant eigenvalue scales as a negative power of the time, $\lambda_*(t) \sim t^{\nu-1}$, $0 \leqslant \nu < 1$, so that $e^{-\lambda_*(t)t} \sim e^{-t^{\nu}}$, a stretched-exponential relaxation to equilibrium. This stretched-exponential relaxation is easily demonstrated numerically (see below). The eigenvalue calculation will be sketched in the Supplemental Material (SM) [45]. We turn now instead to the rate-function calculation. Most strikingly, we shall see that the power of t in the stretched exponential can be obtained immediately from our scaling ansatz for the rate function.

Large deviation formalism. From Eq. (1) we can write the PDF, up to preexponential factors, as $P(x,t) \sim e^{-t^{\nu}\mathcal{I}(z)}$. Inserting this ansatz into the FPE (2), we find that in the long-time limit

$$\frac{z\gamma\mathcal{I}'(z) - \nu\mathcal{I}(z)}{t^{1-\nu}} = \frac{\mathcal{I}'(z)^2}{t^{2\gamma-2\nu}} - \frac{V_0}{k_B T}\frac{\alpha}{z^{1-\alpha}}\frac{\mathcal{I}'(z)}{t^{(2-\alpha)\gamma-\nu}}. \tag{4}$$

We impose that the time dependence of all terms is the same, namely, $1 - \nu = 2\gamma - 2\nu = (2-\alpha)\gamma - \nu$, and find that the scaling exponents are

$$\nu = \frac{\alpha}{2-\alpha} \quad \text{and} \quad \gamma = \frac{1}{2-\alpha}. \tag{5}$$

With these exponents, both the exponent of the Boltzmann-Gibbs solution, $V(x)/k_B T = V_0/k_B T x^{\alpha} = t^{\nu} V_0/k_B T z^{\alpha}$, and of free diffusion, $x^2/4Dt = t^{\nu} z^2/4D$, are compatible with our scaling.

The rate function can be found by solving the nonlinear differential equation (4), which now reads

$$\mathcal{I}'(z)^2 - \left(\frac{V_0}{k_B T}\frac{\alpha}{z^{1-\alpha}} + \frac{z}{2-\alpha}\right)\mathcal{I}'(z) + \frac{\alpha\mathcal{I}(z)}{2-\alpha} = 0. \tag{6}$$

When we consider the large-z limit, the rate-function solution will assume the form $\mathcal{I}(z) \approx \xi_0 z^{\mu_0}$, where μ_0 and ξ_0 must be determined. Plugging $\mathcal{I}(z)$ into Eq. (6) in the limit of large z, we have

$$\xi_0\mu_0^2 z^{\mu_0-2} - \frac{V_0}{k_B T}\alpha\mu_0 z^{\alpha-2} \sim \left(\frac{\mu_0 - \alpha}{2-\alpha}\right). \tag{7}$$

There are two possible solutions for this equation. First, we have $\mu_0 = \alpha$, leading to $\mathcal{I}(z) = V_0 z^{\alpha}/k_B T$, i.e., the aforementioned Boltzmann-Gibbs state, which is a solution of Eq. (6) for all z. Second, we have $\mu_0 = 2$ and $\xi_0 = 1/4$, which is equivalent to large-z diffusive behavior. We emphasize that these are the only possible asymptotic solutions of Eq. (6). Both these behaviors are necessary. The Boltzmann-Gibbs state is a possible time-independent solution of the problem, when the initial state is the equilibrium state. However, under any initial conditions that decay with x faster than the Boltzmann-Gibbs state and for any finite time t, we cannot expect the Boltzmann-Gibbs state to describe the whole PDF. The particles cannot spread faster than what is permitted by diffusion. Since $F(x) \to 0$ as $x \to \infty$, we expect diffusive behavior at large $|x|$, consistent with the second asymptotic behavior.

The next step is to solve Eq. (6) globally. Since Eq. (6) is a second-order polynomial in $\mathcal{I}'(z)$, we have in fact two different options for the ordinary differential equation (ODE):

$$\mathcal{I}'(z) = \frac{1}{2}\left(\frac{V_0}{k_B T}\frac{\alpha}{z^{1-\alpha}} + \frac{z}{2-\alpha}\right) \pm \frac{1}{2}\sqrt{\left(\frac{V_0}{k_B T}\frac{\alpha}{z^{1-\alpha}} + \frac{z}{2-\alpha}\right)^2 - \frac{4\alpha\mathcal{I}(z)}{2-\alpha}}. \tag{8}$$

These two ODEs give rise to two smooth solutions that cross at a critical point z_c, at which the square root vanishes. One solution has the positive sign of the square root for $z < z_c$ and

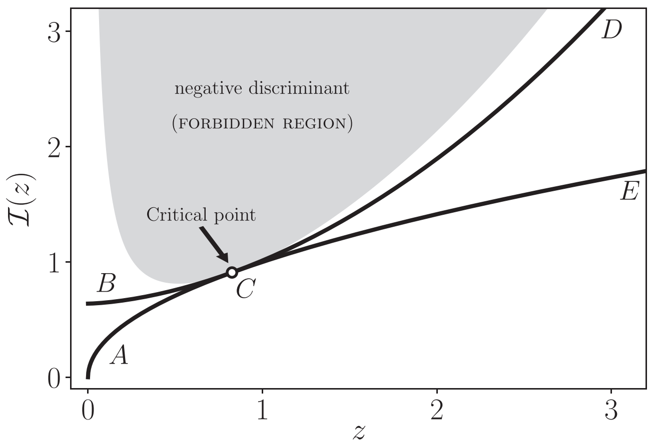

FIG. 1. All possible rate functions, defined by Eq. (1), which are solutions of the differential equation in Eq. (6), vs the scaled position $z \equiv x/t^\gamma$ [the scaled exponents defined in Eq. (5)] for $\alpha = 1/2$. The rate function has two low-z and two high-z branches, leading to four different possible forms. The region where the discriminant of Eq. (8) is negative is highlighted in gray.

the negative sign for $z > z_c$ and the other with the opposite choices. Interestingly, two other solutions are also possible, where the sign does not switch, and which have a jump in $\mathcal{I}''$, leaving us with four possible descriptions, two for $z < z_c$ and two for $z > z_c$, as shown in Fig. 1. The next task is to uncover the physical content of these rate-function branches.

Boltzmann-Gibbs thermal initial condition. As noted above, if we were to start at time $t = 0$ with the thermal state in all of space, the state would remain unchanged for all time. In Fig. 1, this is shown as the curve *ACE*. The square root in Eq. (8) vanishes at the critical point z_c,

$$z_c = \left(\frac{\alpha(2-\alpha)V_0}{k_B T}\right)^{1/(2-\alpha)}. \tag{9}$$

The pure thermal state is obtained when we switch from positive ($z < z_c$) to negative ($z > z_c$) in Eq. (8).

Localized initial condition. Our goal is to associate the solutions shown in Fig. 1 with classes of initial conditions and with parity. For an initially localized packet of particles, we expect the large-z behavior to be diffusive rather than Boltzmann-Gibbs. However, for small z, we expect the behavior to match Boltzmann-Gibbs, so that the Boltzmann-Gibbs regime in x expands as t^γ. Keeping the positive sign of the square-root for $z > z_c$ leads to the desired diffusivelike large-z behavior. The resulting singularity in $\mathcal{I}''$ is precisely the dynamical phase transition. The resulting curve, *ACD* in Fig. 1, describes the localized initial condition.

We can write odd/even PDFs using distinct rate functions as

$$P_{\text{even}} \sim e^{-t^\nu \mathcal{I}_{\text{even}}(z)} \quad \text{and} \quad P_{\text{odd}} \sim e^{-t^\nu \mathcal{I}_{\text{odd}}(z)}. \tag{10}$$

If the particles start at the origin ($x_0 = 0$), then by symmetry $P_{\text{odd}}(x,t) = 0$, since $V(x)$ is even and so all odd moments vanish, as they do in equilibrium. On the other hand, for $x_0 \neq 0$, the odd part is present, $P_{\text{odd}} = [P(x,t) - P(-x,t)]/2$, and is described by the curve *BCD*. We then write that $\mathcal{I}_{\text{odd}}(z) \equiv \mathcal{I}_{BCD}(z)$, which tends to a constant value $\mathcal{I}_{\text{odd}}(0)$ as z approaches zero (see Fig. 1). Therefore, we have that $P_{\text{odd}}(x,t)$ has an upper bound that decays as $e^{-\mathcal{I}_{\text{odd}}(0)t^\nu}$, indicating that the odd contributions will decay as a stretched exponential. Curve *BCE* describes the contribution from the continuum modes. This contribution is obtained by subtracting from $P(x,t)$ the Boltzmann-Gibbs solution, $P^* \equiv P - P_{\text{BG}}$. At large x, this results in the negative of the Boltzmann-Gibbs solution, as the full solution is small. Here, the stretched-exponential relaxation of the even moments of x to their equilibrium values is controlled by P^*. The rate function, *BCE* in Fig. 1, also displays a dynamical phase transition at the critical point. Finally, the even part, $P_{\text{even}} = [P(x,t) + P(-x,t)]/2$, is described by the *ACD* rate function, $\mathcal{I}_{\text{even}}(z) \equiv \mathcal{I}_{ACD}(z)$. This solution also captures the leading behavior of the density $P(x,t)$ for localized initial conditions.

We presented the four different scenarios for the rate function represented by branches in Fig. 1. Which scenario is the relevant one is based on the choice of the initial condition and the parity. We now use finite-time numerical integration of the FPE to show that, using Eq. (1) (adapted for finite times), the results converge to the expected rate functions. In Fig. 2(a), for localized initial conditions, we show the numerical convergence to the rate function *ACD*, while in Fig. 2(b) we show the derivative of the curve *ACD*. The derivative clearly shows the nonanalytical behavior at the point z_c. In Fig. 2(c), we compare our long-time prediction for $\mathcal{I}_{\text{odd}}(z)$ [$I_{BCD}(z)$] with numerical results ($t^{-\nu} \log P_{\text{odd}}$, with P_{odd} obtained numerically), showing clear convergence.

In summary, we find that two of the rate functions are completely analytical. Those are the Boltzmann-Gibbs (curve *ACE*) and the odd rate functions (curve *BCD*). The other two possibilities, the localized initial condition rate function (curve *ACD*) and the continuum mode rate function (curve *BCE*), have a nonanalytical behavior, and therefore a dynamical phase transition, at the critical point z_c.

Remark on the notation and prefactors. We highlight that the rate functions defined in Eq. (10) satisfy $\mathcal{I}_{\text{even/odd}}(z) = \mathcal{I}_{\text{even/odd}}(-z)$ as these functions are even. Further, they do not depend explicitly on the initial conditions. The parity of $P_{\text{even/odd}}$ is determined by the preexponential factors. The exponential prefactors of P_{odd} will depend on the initial condition, since for symmetric initial conditions, the whole odd part must vanish. The prefactor is obtained using the WKB method in the SM.

Anomalous relaxation. Here, we study the relaxation properties of the system, focusing on the first moment of the position x, starting with an asymmetric initial condition ($x_0 \neq 0$). Because this observable, x, is odd, the only nonzero contribution comes from the asymmetric part of the PDF. The odd part of the PDF can be written using $\mathcal{I}_{\text{odd}}$, up to preexponential factors, as shown in Eq. (10). We obtain, up to preexponential factors, the stretched-exponential characteristic of the mean as

$$\langle x \rangle = \int_{-\infty}^{\infty} x\, P_{\text{odd}}(x,t) dx \sim e^{-\mathcal{I}_{\text{odd}}(0)t^\nu}. \tag{11}$$

The value of $\mathcal{I}_{\text{odd}}(0)$ governs the anomalous timescale τ of the relaxation. It is possible to obtain this value numerically by integrating Eq. (8) in the correct branch (positive sign). We have obtained an analytical expression through our

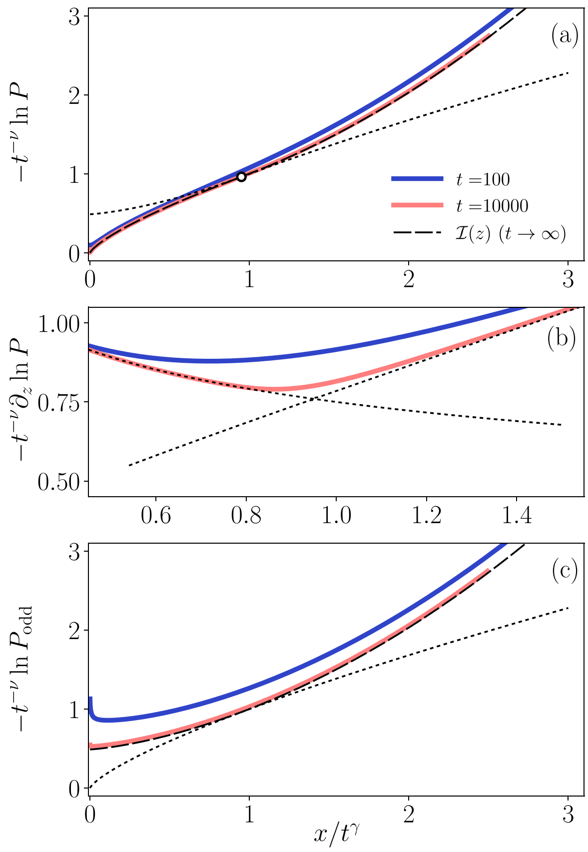

FIG. 2. Comparison between theoretical and numerical (at finite times) rate functions, Eq. (1), as a function of the scaled position $z \equiv x/t^{\gamma}$. The solid lines represent numerical results obtained integrating Eq. (2) at different times, indicated in the legend [(a)] for all panels. The dotted black lines represent all four possible rate functions (see Fig. 1) in (a) and (c) and their derivatives in (b). In (a) we show the clear convergence to the rate function $\mathcal{I}_{ACD}(z)$ and highlight (open circle) the critical transition point z_c. In (b) we show the derivative $\mathcal{I}'(z)$, and the nonanalytical behavior becomes clear. The solution is equivalent to Boltzmann-Gibbs up until the critical point, where the system changes to the free-particle solution for larger values of z. In (c) we have the odd rate functions, where there is no dynamical phase transition. The numerical solutions demonstrate clear convergence towards the expected rate functions. We have used $\alpha = 3/4$, $\ell = 1$, $D = 1$, and $V_0/k_B T = 1$.

eigenfunction calculations (see SM)

$$\frac{1}{\tau^{\nu}} = \mathcal{I}_{\rm odd}(0) = \frac{\left[\sqrt{\pi}\left(\frac{\alpha V_0}{2k_B T}\right)^{\frac{1}{1-\alpha}} \frac{\Gamma\left(\frac{\alpha}{2-2\alpha}\right)}{\Gamma\left(\frac{1}{2-2\alpha}\right)}\right]^{1-\nu}}{\nu^{\nu}(1-\nu)^{1-\nu}}. \qquad (12)$$

It is remarkable that a rate function controls the relaxation, in the sense that it cannot be considered describing a rare event, nor is it particularly hard to measure it. In Fig. 3, the stretched-exponential behavior is shown numerically in the long-time limit. The observed timescale matches our prediction in Eq. (12) and is independent of the odd moment under consideration. The same can be extended for even moments x^{2n} (see SM). In order to obtain a complete expression for the mean in Eq. (11), the rate function is not enough. We must account for the preexponential factor $\mathcal{A}(t)$, that is, $P_{\rm odd} \approx \mathcal{A}(t) x^{1-\alpha} e^{-\mathcal{I}_{\rm odd}(z)t^{\nu}}$.

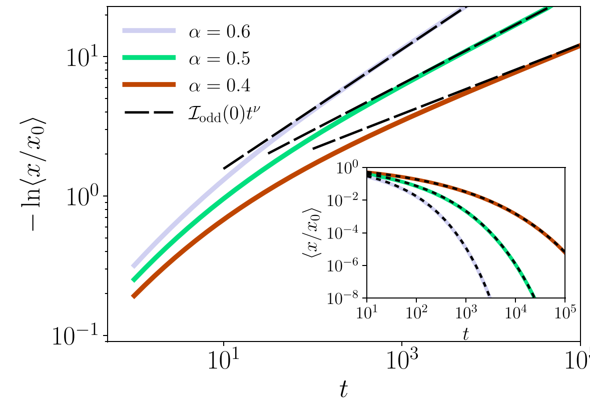

FIG. 3. The log of the numerical ensemble average of the position for a system initialized with a localized condition $P(x, t = 0) = \delta(x - x_0)$ for different values of α (shown in legend). The stretched-exponential behavior is clearly shown for long times, where we compare with $\mathcal{I}_{\rm odd}(0)t^{\nu}$ (dashed black lines), where the anomalous timescale $\mathcal{I}_{\rm odd}(0)$ is obtained in Eq. (12), and $\nu = \alpha/(2-\alpha)$. In the inset, the complete theoretical prediction (dotted black lines), described by Eq. (14), is compared with the numerical simulations (colored lines) for the same exponents α as in the main label. We have used $V_0/k_B T = 1$, $\ell = 1$, and $x_0 = 0.04$.

In the long-time limit, the main contribution to the integral in Eq. (11) arises from the region where x is much smaller than the critical $x_c(t)$, corresponding to the small-z region [46]. For small z, we have $\mathcal{I}_{\rm odd}(z) \approx \mathcal{I}_{\rm odd}(0)[1 + k_B T z^{2-\alpha}/V_0(2-\alpha)^2]$, and the preexponential factor is (see SM)

$$\mathcal{A}(t) = x_0 \frac{k_B T}{\alpha V_0} \frac{\mathcal{I}_{\rm odd}(0) e^{\frac{V(0)}{k_B T}}}{t^{3/2-\nu}} \sqrt{\frac{\gamma - \nu}{4\pi}}. \qquad (13)$$

Note that for the transition value $\alpha = 1$, $\gamma = \nu = 1$, and $\mathcal{A}(t)$ will be null. With the contribution of the prefactor, we obtain, from Eq. (11), the long-time expression for the relaxation,

$$\frac{\langle x\rangle}{x_0} \sim \frac{\mathcal{C}_1\left(\frac{V_0}{k_B T}, \alpha\right)}{t^{\nu^2/2}} e^{-\mathcal{I}_{\rm odd}(0)t^{\nu}}, \qquad (14)$$

where the definition of $\mathcal{C}_1(V_0/k_B T, \alpha)$ is found in the SM. Thus, the time relaxation of the system to equilibrium is through a stretched exponential (multiplied by a power law in time). We show the excellent agreement of Eq. (14) with the numerical results in the inset of Fig. 3.

Discussion. The results we obtained in this Letter are quite general, but nevertheless, many extensions to this work are possible. As a first step in this direction, we studied a case in dimensions higher than one, showing that the main results remain valid. The characteristics of time-averaged observables and the potential link between different branches and singularities in the cumulant generating function warrant attention [47,48]. It is likely that the multivalued nature of the rate function under study, which depends on symmetry and initial condition, is an important feature for other systems. Thus, the appearance of the multivalued rate function in more systems and its relationship with dynamical phase transitions requires further study.

Acknowledgments. The support of Israel Science Foundation's Grant No. 1614/21 is acknowledged. L.D. and E.B. thank Naftali Smith for the insightful conversations.

[1] V. Uchaikin and R. Sibatov, *Fractional Kinetics in Solids* (World Scientific, Singapore, 2013).

[2] R. Kohlrausch, Theorie des elektrischen Rückstandes in der Leidener Flasche, Ann. Phys. (Berlin) **167**, 56 (1854).

[3] J. Klafter and M. F. Shlesinger, On the relationship among three theories of relaxation in disordered systems, Proc. Natl. Acad. Sci. USA **83**, 848 (1986).

[4] C. Kisslinger, The stretched exponential function as an alternative model for aftershock decay rate, J. Geophys. Res.: Solid Earth **98**, 1913 (1993).

[5] O. Flomenbom, K. Velonia, D. Loos, S. Masuo, M. Cotlet, Y. Engelborghs, J. Hofkens, A. E. Rowan, R. J. M. Nolte, M. Van der Auweraer, F. C. de Schryver, and J. Klafter, Stretched exponential decay and correlations in the catalytic activity of fluctuating single lipase molecules, Proc. Natl. Acad. Sci. USA **102**, 2368 (2005).

[6] S. Mukherjee, P. Pareek, M. Barma, and S. K. Nandi, From stretched exponential to power-law: crossover of relaxation in a simple model, arXiv:2307.01801.

[7] L. C. Malacarne, R. S. Mendes, I. T. Pedron, and E. K. Lenzi, Nonlinear equation for anomalous diffusion: Unified power-law and stretched exponential exact solution, Phys. Rev. E **63**, 030101(R) (2001).

[8] A. V. Milovanov, K. Rypdal, and J. J. Rasmussen, Stretched exponential relaxation and ac universality in disordered dielectrics, Phys. Rev. B **76**, 104201 (2007).

[9] R. Metzler and J. Klafter, From stretched exponential to inverse power-law: fractional dynamics, cole-cole relaxation processes, and beyond, J. Non-Cryst. Solids **305**, 81 (2002).

[10] M. Magdziarz and K. Weron, Anomalous diffusion schemes underlying the stretched exponential relaxation. the role of subordinators, Acta Phys. Pol. B **37**, 1617 (2006).

[11] J. Kakalios, R. A. Street, and W. B. Jackson, Stretched-exponential relaxation arising from dispersive diffusion of hydrogen in amorphous silicon, Phys. Rev. Lett. **59**, 1037 (1987).

[12] Z. Wu, W. Kob, W. H. Wang, and L. Xu, Stretched and compressed exponentials in the relaxation dynamics of a metallic glass-forming melt, Nat. Commun. **9**, 5334 (2018).

[13] D. A. Huse and D. S. Fisher, Dynamics of droplet fluctuations in pure and random ising systems, Phys. Rev. B **35**, 6841 (1987).

[14] D. S. Fisher and D. A. Huse, Equilibrium behavior of the spin-glass ordered phase, Phys. Rev. B **38**, 386 (1988).

[15] C. Tang, H. Nakanishi, and J. S. Langer, Droplet model for autocorrelation functions in an Ising ferromagnet, Phys. Rev. A **40**, 995 (1989).

[16] M. I. Freidlin and A. D. Wentzell, *Random Perturbations of Dynamical Systems*, 2nd ed., Grundlehren der mathematischen Wissenschaften (Fundamental Principles of Mathematical Sciences) Vol. 260 (Springer, New York, 1998) (translated from the 1979 Russian original by J. Szücs).

[17] H. Touchette, The large deviation approach to statistical mechanics, Phys. Rep. **478**, 1 (2009).

[18] Y. Baek and Y. Kafri, Singularities in large deviation functions, J. Stat. Mech.: Theory Exp. (2015) P08026.

[19] Y. Baek, Y. Kafri, and V. Lecomte, Dynamical phase transitions in the current distribution of driven diffusive channels, J. Phys. A: Math. Theor. **51**, 105001 (2018).

[20] D. Nickelsen and H. Touchette, Anomalous scaling of dynamical large deviations, Phys. Rev. Lett. **121**, 090602 (2018).

[21] B. Meerson, Anomalous scaling of dynamical large deviations of stationary Gaussian processes, Phys. Rev. E **100**, 042135 (2019).

[22] P. T. Nyawo and H. Touchette, A minimal model of dynamical phase transition, Europhys. Lett. **116**, 50009 (2016).

[23] H. Touchette, Introduction to dynamical large deviations of Markov processes, Physica A **504**, 5 (2018).

[24] R. L. Jack and R. J. Harris, Giant leaps and long excursions: Fluctuation mechanisms in systems with long-range memory, Phys. Rev. E **102**, 012154 (2020).

[25] R. Hurtado-Gutiérrez, P. I. Hurtado, and C. Pérez-Espigares, Spectral signatures of symmetry-breaking dynamical phase transitions, Phys. Rev. E **108**, 014107 (2023).

[26] G. Teza, R. Yaacoby, and O. Raz, Eigenvalue crossing as a phase transition in relaxation dynamics, Phys. Rev. Lett. **130**, 207103 (2023).

[27] M. Janas, A. Kamenev, and B. Meerson, Dynamical phase transition in large-deviation statistics of the Kardar-Parisi-Zhang equation, Phys. Rev. E **94**, 032133 (2016).

[28] T. Nemoto, R. L. Jack, and V. Lecomte, Finite-size scaling of a first-order dynamical phase transition: Adaptive population dynamics and an effective model, Phys. Rev. Lett. **118**, 115702 (2017).

[29] N. R. Smith, Large deviations in chaotic systems: Exact results and dynamical phase transition, Phys. Rev. E **106**, L042202 (2022).

[30] N. R. Smith, Exact short-time height distribution and dynamical phase transition in the relaxation of a Kardar-Parisi-Zhang interface with random initial condition, Phys. Rev. E **106**, 044111 (2022).

[31] N. R. Smith, Anomalous scaling and first-order dynamical phase transition in large deviations of the Ornstein-Uhlenbeck process, Phys. Rev. E **105**, 014120 (2022).

[32] S. Mukherjee and N. R. Smith, Dynamical phase transition in the occupation fraction statistics for noncrossing Brownian particles, Phys. Rev. E **107**, 064133 (2023).

[33] R. Gutiérrez, A. Canella-Ortiz, and C. Pérez-Espigares, Finding the effective dynamics to make rare events typical in chaotic maps, Phys. Rev. Lett. **131**, 227201 (2023).

[34] T. Agranov, M. E. Cates, and R. L. Jack, Tricritical behavior in dynamical phase transitions, Phys. Rev. Lett. **131**, 017102 (2023).

[35] H. Risken, *The Fokker-Planck Equation*, Springer Series in Synergetics, Vol. 18 (Springer, Berlin, 1996).

[36] K. Capała and B. Dybiec, Optimization of escape kinetics by reflecting and resetting, Chaos **33**, 103124 (2023).

[37] A. Dhar, A. Kundu, S. N. Majumdar, S. Sabhapandit, and G. Schehr, Run-and-tumble particle in one-dimensional confining potentials: Steady-state, relaxation, and first-passage properties, Phys. Rev. E **99**, 032132 (2019).

[38] Y. Chen, A. Baule, H. Touchette, and W. Just, Weak-noise limit of a piecewise-smooth stochastic differential equation, Phys. Rev. E **88**, 052103 (2013).

[39] S. Sabhapandit and S. N. Majumdar, Freezing transition in the barrier crossing rate of a diffusing particle, Phys. Rev. Lett. **125**, 200601 (2020).

[40] L. Zarfaty, E. Barkai, and D. A. Kessler, Discrete sampling of extreme events modifies their statistics, Phys. Rev. Lett. **129**, 094101 (2022).

[41] D. A. Kessler and E. Barkai, Infinite covariant density for diffusion in logarithmic potentials and optical lattices, Phys. Rev. Lett. **105**, 120602 (2010).

[42] A. Dechant, E. Lutz, E. Barkai, and D. A. Kessler, Solution of the Fokker-Planck equation with a logarithmic potential, J. Stat. Phys. **145**, 1524 (2011).

[43] O. Hirschberg, D. Mukamel, and G. M. Schütz, Approach to equilibrium of diffusion in a logarithmic potential, Phys. Rev. E **84**, 041111 (2011).

[44] O. Hirschberg, D. Mukamel, and G. M. Schütz, Diffusion in a logarithmic potential: Scaling and selection in the approach to equilibrium, J. Stat. Mech.: Theory Exp. (2012) P02001.

[45] See Supplemental Material at http://link.aps.org/supplemental/10.1103/PhysRevE.109.L022102 for technical details about the eigenfunction expansion and its connection to the rate function. The material also includes the derivation of $\mathcal{I}_{\text{odd}}(0)$ in Eq. (12), the derivation of the prefactor in Eq. (13), and the ensemble average in Eq. (14).

[46] The maximum contribution to the integral in Eq. (11) is centered at $x^*(t)$. In the long-time limit, $x^*(t)/x_c(t) \equiv z^*(t)/z_c(t) \sim t^{-\gamma\nu} \to 0$, and therefore, the important region is the $z \to 0$ region.

[47] A. L. Stella, A. Chechkin, and G. Teza, Anomalous dynamical scaling determines universal critical singularities, Phys. Rev. Lett. **130**, 207104 (2023).

[48] A. L. Stella, A. Chechkin, and G. Teza, Universal singularities of anomalous diffusion in the Richardson class, Phys. Rev. E **107**, 054118 (2023).